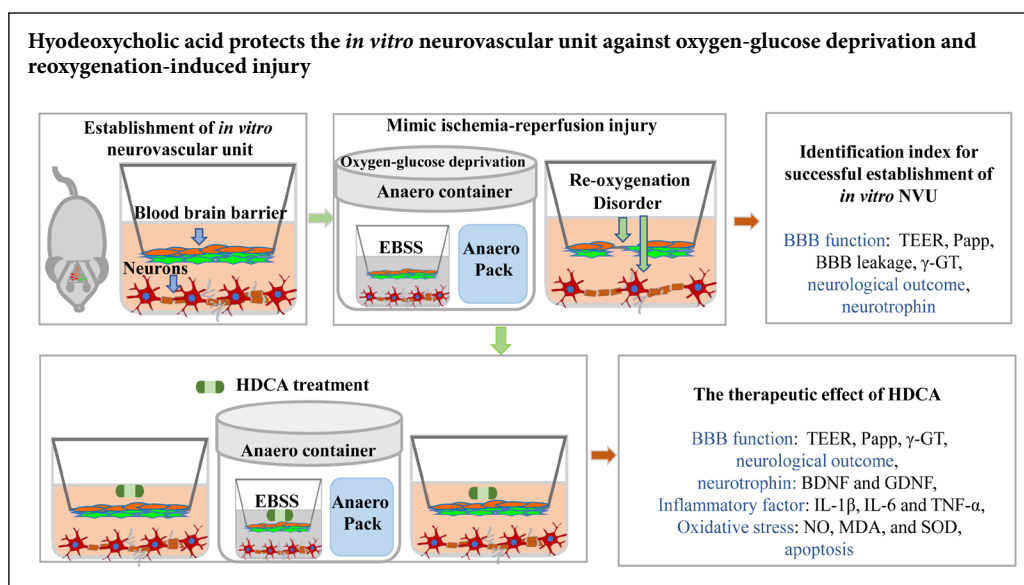


Hyodeoxycholic acid protects the neurovascular unit against oxygen-glucose deprivation and reoxygenation-induced injury *in vitro*

Chang-Xiang Li[‡], Xue-Qian Wang[‡], Fa-Feng Cheng, Xin Yan, Juan Luo, Qing-Guo Wang^{*}
School of Traditional Chinese Medicine, Beijing University of Chinese Medicine, Beijing, China

Funding: This study was supported by the National Natural Science Foundation of China, No. 81430102 (to QGW).

Graphical Abstract



***Correspondence to:**
Qing-Guo Wang, PhD,
wangqg8558@163.com;
Fa-Feng Cheng, PhD,
694639192@qq.com.

#These authors contribute equally to this article.

orcid:
0000-0003-2752-1925
(Qing-Guo Wang)
0000-0002-3409-1196
(Fa-Feng Cheng)

doi: 10.4103/1673-5374.259617

Received: January 28, 2019
Accepted: April 10, 2019

Abstract

Calculus bovis is commonly used for the treatment of stroke in traditional Chinese medicine. Hyodeoxycholic acid (HDCA) is a bioactive compound extracted from calculus bovis. When combined with cholic acid, baicalin and jas-minoidin, HDCA prevents hypoxia-reoxygenation-induced brain injury by suppressing endoplasmic reticulum stress-mediated apoptotic signaling. However, the effects of HDCA in ischemic stroke injury have not yet been studied. Neurovascular unit (NVU) dysfunction occurs in ischemic stroke. Therefore, in this study, we investigated the effects of HDCA on the NVU under ischemic conditions *in vitro*. We co-cultured primary brain microvascular endothelial cells, neurons and astrocytes using a transwell chamber co-culture system. The NVU was pre-treated with 10.16 or 2.54 μ g/mL HDCA for 24 hours before exposure to oxygen-glucose deprivation for 1 hour. The cell counting kit-8 assay was used to detect cell activity. Flow cytometry and terminal deoxynucleotidyl transferase-mediated dUTP nick end labeling were used to assess apoptosis. Enzyme-linked immunosorbent assay was used to measure the expression levels of inflammatory cytokines, including interleukin-1 β , interleukin-6 and tumor necrosis factor- α , and neurotrophic factors, including brain-derived neurotrophic factor and glial cell line-derived neurotrophic factor. Oxidative stress-related factors, such as superoxide dismutase, nitric oxide, malondialdehyde and γ -glutamyltransferase, were measured using kits. Pretreatment with HDCA significantly decreased blood-brain barrier permeability and neuronal apoptosis, significantly increased transendothelial electrical resistance and γ -glutamyltransferase activity, attenuated oxidative stress damage and the release of inflammatory cytokines, and increased brain-derived neurotrophic factor and glial cell line-derived neurotrophic factor expression. Our findings suggest that HDCA maintains NVU morphological integrity and function by modulating inflammation, oxidation stress, apoptosis, and the expression of neurotrophic factors. Therefore, HDCA may have therapeutic potential in the clinical management of ischemic stroke. This study was approved by the Ethics Committee of Experimental Animals of Beijing University of Chinese Medicine (approval No. BUCM-3-2016040201-2003) in April 2016.

Key Words: hyodeoxycholic acid; oxygen glucose deprivation and reoxygenation; blood-brain barrier permeability; anti-oxidative; anti-inflammatory; anti-apoptotic; brain-derived neurotrophic factor; glial cell line-derived neurotrophic factor; ischemic stroke; *in vitro* neurovascular unit

Chinese Library Classification No. R453; R363; R741

Introduction

Stroke is a major cause of mortality and disability, and is a severe socioeconomic burden on health systems worldwide (Quan et al., 2015). According to current data, about 85% of all strokes are ischemic strokes (ISs) (Ovbiagele et al., 2013), which are defined as strokes resulting from insufficient cerebral blood flow caused by an occlusion or stenosis of a brain artery. Multiple pathological processes occur in the ischemic territory in IS, including inflammation, oxidative stress and apoptosis (Schmidt and Minnerup, 2016; Khoshnam et al., 2017). The neurological deficits observed post-stroke are, in general, attributed to the death or dysfunction of neurons. Thus, over the past few decades, efforts to develop neuroprotective agents for IS have focused on these pathogenetic processes in neurons. However, experimental approaches to treat stroke that are solely vasocentric or neurocentric have failed to produce effective stroke therapies (Ginsberg, 2009; Liu and Chopp, 2016).

Recently, the neurovascular unit (NVU) has become a major drug target for IS treatment (Le Moan et al., 2017; Shi et al., 2017). The NVU was proposed as a complex structural and functional unit comprising neurons, glia and pericytes, as well as cells in the blood vessels themselves (Xing et al., 2012). After stroke, the components of the NVU are damaged, impairing its function and contributing to brain damage after stroke (Arai et al., 2011; Tian et al., 2016). Ischemic damage to the NVU disrupts microvascular blood flow and compromises blood-brain barrier (BBB) integrity, which in turn leads to tissue damage and cerebral edema (Dalkara et al., 2016). Therefore, a thorough characterization of NVU structure and function is crucial to understanding the pathology of IS.

Calculus bovis has been widely used for the treatment of stroke for its immunoregulatory and anti-inflammatory properties for thousands of years in traditional Chinese medicine (Jijun et al., 2016). Hyodeoxycholic acid (HDCA) is a bioactive compound extracted from calculus bovis. Our previous studies showed that a combination of active components in calculus bovis can alleviate the damage caused by cerebral IS by inhibiting endoplasmic reticulum stress (Xu et al., 2017). Moreover, HDCA combined with cholic acid, baicalin and jasminoidin prevents ischemia-induced brain injury by suppressing endoplasmic reticulum stress-mediated apoptotic signaling in hypoxia-reoxygenation injury within a time window of 6 hours (Cheng et al., 2012). However, the protective effects of HDCA on the NVU have not been studied. Therefore, in this study, we used an *in vitro* NVU model to examine the protective effects of HDCA on the BBB and neurons in IS.

Materials and Methods

Animals

Specific-pathogen-free neonatal Sprague-Dawley (SD) rat pups, 2–3 weeks ($n = 6$), 3 days ($n = 8$) and 24 hours ($n = 15$) after birth, were purchased from Beijing Weitong Lihua Experimental Animal Technology (license No. SCXK 2016-0006). This study was approved by the Ethics Committee of Experimental Animals of Beijing University of Chinese Medicine (approval No. BUCM-3-2016040201-2003) in April 2016.

Isolation and purification of neurons

Cortical neurons were obtained from newborn (24 hours old) SD rats as described previously (Xue et al., 2013). Briefly, following removal of the meninges and white matter, the purified cerebral cortices were digested with 0.125% trypsin-ethylenediamine tetraacetic acid (Sigma-Aldrich, St. Louis, MO, USA), and then re-suspended in Neurobasal-A medium (Gibco, Grand Island, NY, USA) containing 10% fetal bovine serum (Gibco), 2% B27 (Invitrogen, Carlsbad, CA, USA) and 1% penicillin/streptomycin (Gibco). The cells were seeded at a density of 1×10^6 cells/mL into 0.01% poly-L-lysine (Sigma-Aldrich)-coated dishes, and cultured at 37°C in a 5% CO₂ incubator (Thermo Fisher, Fremont, CA, USA). After 6 hours, the medium was replaced with Neurobasal-A medium containing 2% B27, 0.25% GlutaMAX (Gibco) and 1% penicillin/streptomycin. Primary neurons were characterized by immunofluorescence labeling for microtubule-associated protein 2.

Culturing of primary cortical brain microvascular endothelial cells (BMECs)

BMECs were isolated from 3-day-old SD rats (Xue et al., 2013). Briefly, the meninges and white matter were removed, and the forebrain tissue was centrifuged at $350 \times g$ for 3 minutes. The resulting pellet was resuspended in an equal volume of 25% (g/v) bovine serum albumin and centrifuged at $1600 \times g$ for 5 minutes (4×). The obtained microvessels were digested with type-2 collagenase (1.0 mg/mL, Sigma-Aldrich) for 1 hour and then cultured in Dulbecco's modified Eagle medium/nutrient mixture F-12 (Gibco) containing 20% fetal bovine serum and 1% penicillin/streptomycin. BMECs were collected and seeded on 75 cm² flasks pre-coated with gelatin (2%). Primary BMECs were characterized for von Willebrand factor using fluorescence imaging.

Primary cultures of cortical astrocytes

Astrocytes were obtained from 2–3-week-old SD rats (Park et al., 2017). Briefly, the isolated cells were incubated in flasks pre-coated with poly-L-lysine in Dulbecco's modified Eagle medium/nutrient mixture F12 with 10% fetal bovine serum and 1% penicillin-streptomycin. The fibroblasts were removed after differential attachment. On day 7, the cultures were shaken overnight to remove microglia. Primary astrocytes were characterized by immunofluorescence labeling for glial fibrillary acidic protein.

Immunofluorescence

Cells were fixed for 15 minutes in 4% paraformaldehyde, and then blocked and permeabilized for 1 hour in a solution of 0.3% Triton X-100 (Fisher Scientific) and 10% goat serum (Sigma-Aldrich). Cells were incubated overnight with chicken anti-microtubule-associated protein 2 (1:1000; ab5392, Abcam, Cambridge, UK), mouse anti-glial fibrillary acidic protein (1:200; ab10062, Abcam), rabbit anti-von Willebrand factor (1:100; ab6994, Abcam) and rabbit anti-zonula occludens-1 (1:100; 21773-1-AP, Proteintech, Chicago, IL, USA) antibodies at 4°C. Neurons, astrocytes and BMECs were detected with anti-microtubule-associated protein 2, anti-glial fibrillary acidic protein and anti-von Willebrand

factor antibodies, respectively. Tight junction proteins were labeled with anti-zonula occludens-1 antibody. The following day, the cells were incubated with fluorescently-labeled secondary antibody (Alexa Fluor 647-conjugated goat anti-chicken IgY, 1:300, ab150171, Abcam; FITC-conjugated goat anti-mouse IgG, 1:200, ab6785, Abcam; Alexa Fluor 555-conjugated donkey anti-rabbit IgG, 1:200, ab150074, Abcam; Alexa Fluor 488-conjugated goat anti-rabbit, 1:500, SA00006-2, Proteintech) for 1 hour at 37°C. The cells were imaged on a fluorescence microscope (Fluoview 1000, Olympus, Tokyo, Japan). The number of cell bodies and nuclei were quantified using ImageJ 1.48 (National Institutes of Health, Bethesda, MD, USA). Purity was calculated as the number of cell bodies/the number of nuclei.

Production of the *in vitro* NVU model

Neurons were plated at the bottom of Transwell plates (0.4 µm, Corning, New York, NY, USA) and maintained in Neurobasal-A medium containing 2% B27, 0.25% GlutaMAX and 1% penicillin/streptomycin for at least 48 hours. Astrocytes (3×10^5 cells/cm²) were plated under the insert membrane in a petri dish at 44 hours. After 4 hours, the transwell inserts were inverted and transferred to the plates. At 52 hours, BMECs were plated at a density of 2×10^5 cells/cm² in 0.5 mL of medium on the inside of the gelatin-coated insert. The experiments were initiated 120 hours after establishing the NVU cultures (at 172 hours). The procedure for establishing the *in vitro* NVU model is schematized in **Figure 1** (Xue et al., 2013; Liu et al., 2019). As controls, BMECs, astrocytes or neurons were also cultured alone on the transwell chamber as groups B, A and N, respectively. BMECs were cultured with astrocytes or neurons as the B + A group and the B + N group, respectively. Neurons were cultured with astrocytes as the N + A group. We observed the morphological phenotype of neurons by microscopy (CKX41SF, Olympus).

Detection of BBB leakage

The permeability of the BBB was evaluated by conducting a 4-hour leak test. At 172 hours, 900 µL media was added into the upper insert, and 750 µL media was added into the 12-well plates, for a 0.5-cm liquid level. Inserts without cells were used as the control to detect the formation of tight junctions by BMECs. The volume in the upper insert was measured before and after 4 hours of incubation (Xue et al., 2013).

Sodium fluorescein permeability measurement

We evaluated the apparent permeability (Papp) for the small molecule sodium fluorescein (SF; 376 Da) to detect the formation of tight junctions by BMECs. SF (100 µg/mL) was added in the upper chamber. A 100-µL volume was collected from the lower chamber at 15, 30, 45 and 60 minutes, and then replenished with pre-equilibrated culture media. The absorbances of the samples were measured using a fluorescence spectrophotometer (FLUOstar Omega, BMG Labtech, Offenburg, Germany). $Papp = (dM/dt)/(A \cdot C)$, where dM/dt is the cumulative measured fluorescence intensity in the plate per unit time, A refers to the bottom area of the insert (1.12 cm²), and C refers to the SF intensity in the upper insert (Shaik

et al., 2013; Liu et al., 2014).

Transendothelial electrical resistance measurement

Transendothelial electrical resistance (TEER; $\Omega \cdot \text{cm}^2$) was measured using a resistance meter (ERS-2, Millipore, Billerica, MA, USA). The overall resistance can characterize the formation of a tight endothelial cell monolayer. The cultures were allowed to equilibrate at 25°C for 20 minutes before detection. The TEER of the inserts was calculated by subtracting the resistance of the control insert from that of the insert and multiplying the difference by the area of the insert.

Ischemic insult to the NVU and drug treatment

As shown in Figure 1, to mimic *in vivo* ischemic conditions, the medium was replaced with deoxygenated Earle's balanced salt solution without glucose (Leagene Biotech Co., Beijing, China) at 196 h. Then, the cultures were transferred into an Anaero container with an Anaero Pack and oxygen indicator (Mitsubishi, Tokyo, Japan) for 1 hour to produce oxygen-glucose deprivation (OGD). Following the anaerobic treatment, OGD was terminated with fresh medium, and the cultures were transferred to a normoxic incubator at 37°C for 24 hours to mimic reoxygenation (R). The cocultures given this treatment were defined as the model group. The control group was incubated in complete medium without OGD/R.

HDCA was purchased from the National Institute for the Control of Pharmaceutical and Biological Products (Beijing, China). The protective effects of HDCA against OGD/R injury in the NVU model were evaluated using the most appropriate dose for the particular type of cell. The BMECs, neurons and astrocytes were seeded in 96-well plates. The solution of HDCA (0.32, 0.64, 1.27, 2.54, 5.08, 10.16, 20.31, 40.63, 81.25 µg/mL) was prepared in Earle's balanced salt solution without glucose or complete medium. Cells were pretreated with the different concentrations of HDCA for 24 hours prior to and during the OGD/R injury procedure.

The solution of HDCA (10.16 and 2.54 µg/mL) was prepared. The NVU model cultures were divided into four groups: (1) control group; (2) HDCA-H group (HDCA, 10.16 µg/mL); (3) HDCA-L group (HDCA, 2.54 µg/mL); (4) model group. The cocultures in the HDCA-H and HDCA-L groups were pretreated with HDCA for 24 hours, and then treated with HDCA during OGD/R (Liao et al., 2016).

Measurement of cell viability in the NVU model

For Cell counting kit-8 assays (CK04-500, Dojindo Molecular Technologies, Inc., Tokyo, Japan), cultures were incubated in culture medium containing 10% (v/v) Cell counting kit-88 solution for 1.5 hours. Absorbance was measured at 450 nm using a microplate reader (Biotek, Winooski, VT, USA).

Flow cytometric analysis of apoptosis in the NVU model

The annexin V apoptosis detection kit (KGA105-KGA108, Kegen, Nanjing, China) was used to assess apoptosis. Cells were digested with ethylenediamine tetraacetic acid-free enzymes and harvested. The cells were mixed with 400 µL binding buffer, and then, 4 µL annexin V-FITC and 4 µL

propidium iodide were added and incubated for 10 minutes. Cells were immediately examined on a FACSCalibur flow cytometer and analyzed with CellQuest software (BD Biosciences, Franklin, NJ, USA). We then quantified the percentage of apoptotic cells in the Q2 (early apoptosis), Q4 (late apoptosis) and Q1 (necrosis) quadrants.

Terminal deoxynucleotidyl transferase-mediated dUTP nick end labeling (TUNEL) assay in the NVU model

TUNEL assay (KGA7071/KGA7072/KGA7073, Kegen) was performed according to the manufacturer's instructions. TUNEL-positive neurons (red) were detected using a fluorescence microscope (Fluoview 1000, Olympus). Data were analyzed with ImageJ 1.48 (National Institutes of Health), and the apoptotic rate was expressed as a percentage of propidium iodide-stained nuclei.

Enzyme-linked immunosorbent assay (ELISA) analysis of the NVU model

Interleukin-1 β (LH-E10099RA, Wuhan Liu he Biotechnology Co., Wuhan, China), interleukin-6 (LH-E10103RA, Wuhan Liu he Biotechnology Co.), tumor necrosis factor- α (KE20001, Proteintech), brain-derived neurotrophic factor (BDNF) (LH-E10031RA, Wuhan Liu he Biotechnology Co.) and glial cell line-derived neurotrophic factor (GDNF) (ELR-GDNF-1, Raybiotech, Guangzhou, China) were measured using ELISA kits according to the manufacturers' instructions. Absorbance was measured at 450 nm using a microplate reader (Biotek).

Assay for superoxide dismutase, nitric oxide, malondialdehyde and γ -glutamyltransferase in the NVU model

Nitric oxide (NO; E1030, Applygen Institute, Beijing, China) level, malondialdehyde content, superoxide dismutase activity and γ -glutamyltransferase activity were tested using kits according to the manufacturers' instructions. The malondialdehyde (A003-1), superoxide dismutase (A001-3) and γ -glutamyltransferase (c017-2) assays were purchased from Jiancheng Bioengineering Institute (Nanjing, China). Absorbance was measured using a microplate reader (Biotek).

Statistical analysis

All experiments were performed in triplicate. All data are expressed as the mean \pm standard deviation (SD). Multiple comparisons were performed using one-way analysis of variance followed by the least significant difference test using SPSS 20.0 (IBM, Armonk, NY, USA). Values of $P < 0.05$ were considered statistically significant.

Results

BBB function and neuronal morphological phenotype in the NVU model

Cell purity was determined by immunofluorescence. The purity of neurons, astrocytes and BMECs from the rat brain were $> 93\%$, $> 99\%$ and 100% , respectively (**Figure 2a–c**). We then established an *in vitro* NVU model and measured BBB properties. BMECs formed a monolayer at the cell boundaries and expressed zonula occludens-1 by immu-

no-fluorescence (**Figure 2d**). In addition to the presence and distribution of tight junction proteins, TEER measurements and the endothelial permeability coefficient for SF were used to compare the physical properties of the *in vitro* BBB model in the various cultures. The NVU model reached a maximum TEER at 120 hours, which was significantly higher than the values in the monoculture system or in BMECs co-cultured either with neurons or astrocytes ($P < 0.01$; **Figure 2e**). The low paracellular Papp of SF in the co-culture system confirms the formation of an impermeable barrier *in vitro*. The permeability coefficients of SF in the NVU system were minimal compared with those in the single culture of BMECs and in BMECs co-cultured with neurons or astrocytes ($P < 0.01$; **Figure 2f**). The volume of the medium in the upper inserts did not change in the various cultures compared with the insert without cells ($P < 0.01$; **Figure 2h**). γ -Glutamyltransferase activity, which is a reliable marker of the BBB and is abundant on the apical surface of endothelial cells (Liu et al., 2011; Fan et al., 2015), reached a higher value in the triple cell co-culture NVU model than in the other culture systems ($P < 0.01$; **Figure 2g**). Moreover, neuronal morphological changes were observed. As shown in **Figure 2i**, neurons acquired a more mature morphological phenotype when cultured with astrocytes or BMECs than when cultured alone. Neuronal axons were fully extended in the NVU model, forming a complex neuronal network. Moreover, neuronal cell bodies were smoother and rounder than in the other culture systems.

Protective effects of HDA on astrocytes and neurons in the NVU exposed to OGD/R

We further explored the impact of astrocytes and BMECs on neurons in the NVU system exposed to OGD (1 hour)/R (24 hours). OGD/R induced widespread apoptosis in all cell types, and the proportion of necrotic and apoptotic cells was greatly reduced in the *in vitro* NVU system compared with the other culture systems ($P < 0.01$; **Figure 3a**). Furthermore, neuronal survival was greater in the triple co-culture system, compared with cultures of neurons alone or neurons co-cultured with either BMECs or astrocytes. Therefore, the *in vitro* NVU model is useful for studying the roles and functions of the various cell types under OGD/R conditions.

We examined the protective effects of various HDCA concentrations on the different cell types to identify the optimal dose. For all cell types, HDCA provided dose-dependent protection at concentrations of 1.27–81.25 $\mu\text{g}/\text{mL}$, with significantly different effects in the OGD/R model ($P < 0.01$). We found that 10.16 $\mu\text{g}/\text{mL}$ HDCA was the optimal dose, with a more significant protective effect than 2.54 $\mu\text{g}/\text{mL}$ HDCA ($P < 0.01$; **Figure 3b–d**). Thus, our NVU system is useful for assessing the effects of therapeutic compounds on neural function after crossing the endothelial barrier.

HDA improves BBB function and neuronal morphological phenotype in the NVU after OGD/R

Next, we analyzed the protective effect of HDCA on the BBB. As shown in **Figure 4a–c**, compared with control conditions, OGD/R significantly increased the Papp for SF ($P < 0.01$; **Figure 4b**) and significantly reduced the TEER value

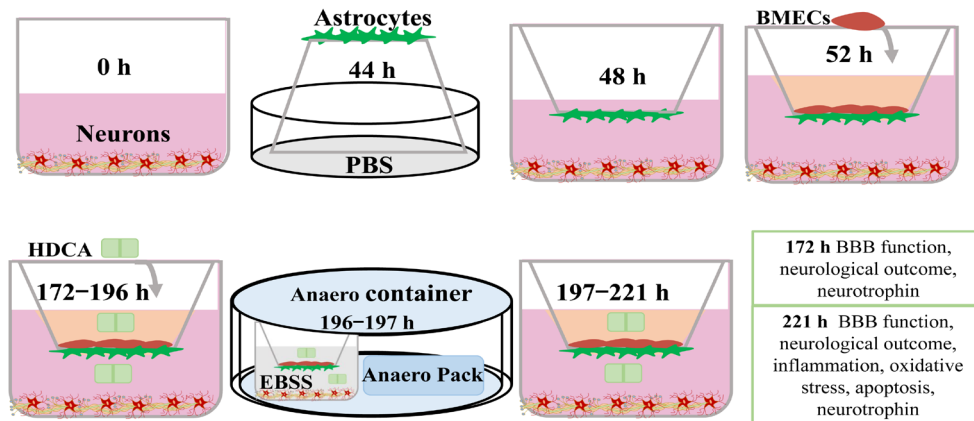


Figure 1 Schematic of the study design and data outputs.

BMECs: Brain microvascular endothelial cells; HDCA: hyodeoxycholic acid; EBSS: Earle's balanced salt solution without glucose; BBB: blood-brain barrier; PBS: phosphate-buffered saline; h: hour(s).

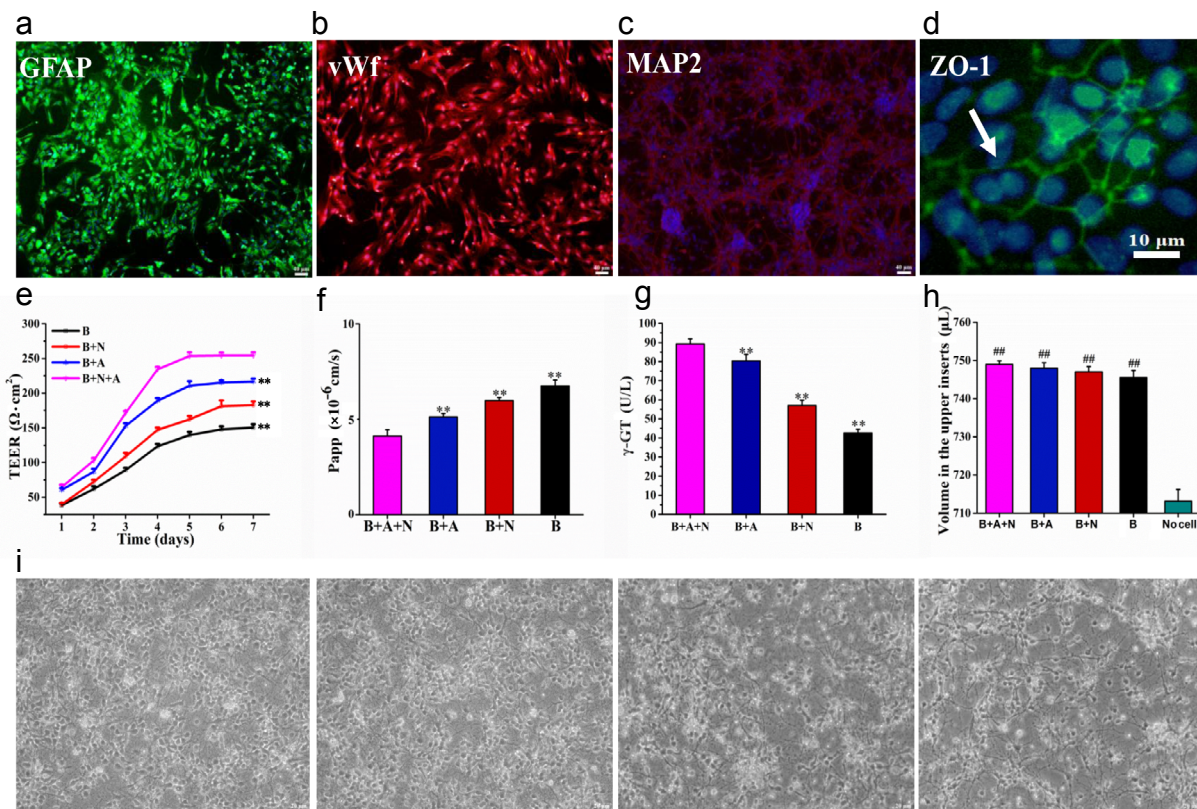


Figure 2 Morphological and functional features of the *in vitro* neurovascular unit (NVU) model.

(a–d) Immunostaining for all cell types in the NVU model. (a) Astrocytes stained for glial fibrillary acidic protein (GFAP) (green, Alexa Fluor 647). (b) Brain microvascular endothelial cells (BMECs) stained for von Willebrand factor (vWF) (red, Alexa Fluor 555). (c) Neurons stained for microtubule-associated protein 2 (MAP-2) (red, FITC). (d) Zonula occludens-1 (ZO-1) immunoreactivity showing tight junctions (green, Alexa Fluor 488). (e) Transendothelial electrical resistance (TEER) values over 7 days. (f–h) The permeability coefficient of sodium fluorescein (f), expression of γ -glutamyltransferase (γ -GT) (g), and volume of the medium in the upper inserts (h) in the B + A + N, B + A, B + N, and B groups. (i) Neuronal morphology in the B + A + N, B + A, B + N, and B groups. Neurons in the N + A + B group exhibit a more mature morphological phenotype. Data are expressed as the mean \pm SD. $**P < 0.01$, vs. B + A + N group; $##P < 0.01$, vs. no cell group (one-way analysis of variance followed by the least significant difference test). All experiments were performed in triplicate. Scale bars: 40 μ m in a–c, 10 μ m in d, 20 μ m in i. B + A + N group: BMECs cultured with astrocytes and neurons; B + A group: BMECs cultured with astrocytes; B + N group: BMECs cultured with neurons; B group: BMECs cultured alone in the transwell chamber.

and γ -glutamyltransferase activity ($P < 0.01$; **Figure 4a** and **c**). These findings are indicative of BBB damage. HDCA treatment markedly improved the integrity of the BBB following OGD/R ($P < 0.01$). As shown in **Figure 4d**, microscopic imaging analysis revealed that the number of neurons in the model group was much less than that in the control group. Furthermore, neuronal cell bodies were irregular and neurites were shorter and thinner in the OGD/R group. HDCA significantly protected against these pathomorphological changes to neurites and neuronal cell bodies.

HDCA reduces inflammatory and oxidative damage to the NVU after OGD/R

We examined the effect of HDCA on the release of tumor necrosis factor- α , interleukin- 1β and interleukin-6. As shown in **Figure 5a–c**, OGD/R induced a significant increase in inflammatory cytokines, compared with the control group. HDCA significantly inhibited the release of these cytokines in a dose-dependent manner ($P < 0.01$). As shown in **Figure 5d–f**, after OGD/R, superoxide dismutase decreased and malondialdehyde and NO increased significantly compared with the control group ($P < 0.01$). HDCA dose-dependently protected against this increase in oxidative stress induced by OGD/R ($P < 0.01$).

HDCA inhibits apoptosis in the NVU after OGD/R

We next assessed the effects of HDCA on OGD/R-induced neuronal apoptosis. Compared with the model group, the proportion of apoptotic cells was significantly lower in the groups given HDCA treatment ($P < 0.01$). Furthermore, HDCA pretreatment reduced OGD/R-induced apoptosis in neurons in a dose-dependent manner ($P < 0.01$; **Figure 6**).

HDCA increases the expression of BDNF and GDNF in the NVU after OGD/R

Finally, we examined effects of HDCA on key neurotrophic factors. BDNF and GDNF levels were higher in the NVU system than in the other culture systems under normal conditions ($P < 0.01$; **Figure 7a** and **c**). Moreover, BDNF and GDNF were expressed and secreted more in the model group than in the control group ($P < 0.01$; **Figure 7b** and **d**). HDCA treatment further increased GDNF and BDNF expression and secretion levels in a dose-dependent manner ($P < 0.01$).

Discussion

Establishing an *in vitro* NVU model that effectively mimics the *in vivo* conditions is key to studying its role in diseases such as IS. We established the *in vitro* NVU system consisting of neurons, astrocytes and BMECs. The neuronal morphological phenotype, neuronal apoptosis and function of the BBB in the *in vitro* cortical NVU were assessed and compared with monocultures as well as two different double cell co-culture systems under physiological and pathological conditions. The main findings and their implications are summarized below. First, neuronal cells show a more mature morphological phenotype, as well as properties indicating BBB integrity, including expression of tight junction components, a relatively lower permeability, a relatively higher metabolic enzyme activity, and greater electrical resistance

in the NVU co-culture system consisting of BMECs, astrocytes and neurons. In addition, TEER and the permeability coefficient, gold standard indices of BBB function, indicated good integrity and permeability of the *in vitro* NVU system. Second, the proportion of apoptotic neurons in the cortical NVU system was lower than that in the monoculture system or the double cell co-culture systems. Notably, a previous study showed that BMECs and astrocytes had a substantial protective effect on neurons after IS (Liu and Chopp, 2016; Wu et al., 2016; Morrison and Filosa, 2019). Third, expression of secretory proteins by astrocytes and neurons, including GDNF and BDNF, which are key neurotrophins, were increased in the *in vitro* NVU system, compared with the monoculture system or the double cell co-culture systems. This indicates neuroprotection, as both GDNF and BDNF promote neuronal maturation by promoting increased cell size and neurite length (Choo et al., 2017; Ibáñez and Andressoo, 2017). Therefore, the *in vitro* NVU models are more suitable for studying the effects of neuroprotective agents on neural function after crossing the endothelial barrier than the other culture models assessed in this study.

The NVU model was therefore used to study the effects of HDCA treatment. Using this model, we show, for the first time, that HDCA treatment i) significantly improves the integrity of the BBB and neuronal morphology, ii) significantly decreases oxidative stress and inflammatory changes, and iii) exerts a dose-dependent neuroprotective effect by suppressing apoptosis and damage to the NVU after OGD/R. There are several possible mechanisms by which HDCA may convey neuroprotection. HDCA is a secondary bile acid, and several bile acids (e.g., cholic acid and ursodeoxycholic acid) have anti-apoptotic and anti-inflammatory effects (Hua et al., 2009; Hu et al., 2012; Tschirner et al., 2012; Dosa et al., 2013). Furthermore, HDCA can inhibit the absorption of intestinal cholesterol and exert anti-atherosclerotic effects, further reducing the risk of cerebral IS (Shih et al., 2013; Leng et al., 2016). In addition to these actions, we found here that HDCA increases the expression of BDNF and GDNF. These factors act through separate neuroprotective signaling pathways, suggesting that HDCA may have broad neuroprotective effects. Tyrosine kinase receptor B (TrkB) is an endogenous receptor for BDNF, and the BDNF/TrkB complex can activate the mitogen-activated protein kinase/extracellular signal-regulated kinase, phospholipase C γ and phosphatidylinositol 3-kinase pathways to promote neuronal survival after OGD/R (Liu et al., 2017; Tejada and Díaz-Guerra, 2017; Kowiański et al., 2018). GDNF protects neurons via binding to the cognate GFR α receptor, which then forms the GDNF/GFR α 1/RET complex to activate Ras/mitogen-activated protein kinase and phosphatidylinositol 3-kinase pathways to promote neuronal survival during ischemia (Saarma and Sariola, 1999; Duarte et al., 2012; Ibáñez and Andressoo, 2017).

In summary, we established an *in vitro* model of the NVU. This model showed that HDCA has anti-oxidative, anti-inflammatory and anti-apoptotic effects, which significantly reduced NVU damage and improved BBB integrity. We speculate that HDCA may provide neuroprotection by promoting the release of neurotrophic factors. We will examine this possibility in future studies. Furthermore, we will use

human cell lines in future studies to better model the NVU in humans. Nonetheless, taken together, our findings suggest that HDCA may have therapeutic potential in the clinical management of human IS.

Author contributions: Study concept and design: CXL, QGW, XQW, FFC; paper writing and language polishing: CXL, XY; experiment implementation: CXL, JL. All authors approved the final version of this paper.

Conflicts of interest: We declare that we have no competing financial interests exist that could inappropriately influence this work.

Financial support: This study was supported by the National Natural Science Foundation of China, No. 81430102 (to QGW). The funding body played no role in the study design, collection, analysis and interpretation of data, in the writing of the report, or in the decision to submit the paper for publication.

Institutional review board statement: This study was approved by the Ethics Committee of Experimental Animals of Beijing University of Chinese Medicine (approval No. BUCM-3-2016040201-2003) in April 2016.

Copyright license agreement: The Copyright License Agreement has been signed by all authors before publication.

Data sharing statement: Datasets analyzed during the current study are available from the corresponding author on reasonable request.

Plagiarism check: Checked twice by iThenticate.

Peer review: Externally peer reviewed.

Open access statement: This is an open access journal, and articles are distributed under the terms of the Creative Commons Attribution-Non-Commercial-ShareAlike 4.0 License, which allows others to remix, tweak, and build upon the work non-commercially, as long as appropriate credit is given and the new creations are licensed under the identical terms.

Open peer reviewers: Lorenzo Romero-Ramírez, Hospital Nacional de Paraplégicos, Spain; Farid Mena, Internal Medicine and Nanomedicine, USA.

Additional file: Open peer review reports 1 and 2.

References

- Arai K, Lok J, Guo S, Hayakawa K, Xing C, Lo EH (2011) Cellular mechanisms of neurovascular damage and repair after stroke. *J Child Neurol* 26:1193-1198.
- Cheng F, Zhong X, Lu Y, Wang X, Song W, Guo S, Wang X, Liu D, Wang Q (2012) Refined Qingkailing protects MCAO mice from endoplasmic reticulum stress-induced apoptosis with a broad time window. *Evid Based Complement Alternat Med* 2012:567872.
- Choo M, Miyazaki T, Yamazaki M, Kawamura M, Nakazawa T, Zhang J, Tanimura A, Uesaka N, Watanabe M, Sakimura K, Kano M (2017) Retrograde BDNF to TrkB signaling promotes synapse elimination in the developing cerebellum. *Nat Commun* 8:195.
- Dalkara T, Alarcon-Martinez L, Yemisci M (2016) Role of Pericytes in Neurovascular unit and stroke. In: *Non-neuronal mechanisms of brain damage and repair after stroke* (Chen J, Zhang JH, Hu X, eds), pp 25-43. Cham: Springer International Publishing.
- Dosa PI, Ward T, Castro RE, Rodrigues CM, Steer CJ (2013) Synthesis and evaluation of water-soluble prodrugs of ursodeoxycholic acid (UDCA), an anti-apoptotic bile acid. *ChemMedChem* 8:1002-1011.
- Duarte EP, Curcio M, Canzoniero LM, Duarte CB (2012) Neuroprotection by GDNF in the ischemic brain. *Growth Factors* 30:242-257.
- Fan X, Chai L, Zhang H, Wang Y, Zhang B, Gao X (2015) Borneol depresses p-glycoprotein function by a NF-kappaB signaling mediated mechanism in a blood brain barrier in vitro model. *Int J Mol Sci* 16:27576-27588.
- Ginsberg MD (2009) Current status of neuroprotection for cerebral ischemia: synaptic overview. *Stroke* 40:S111-114.
- Hu Z, Ren L, Wang C, Liu B, Song G (2012) Effect of chenodeoxycholic acid on fibrosis, inflammation and oxidative stress in kidney in high-fructose-fed Wistar rats. *Kidney Blood Press Res* 36:85-97.
- Hua Q, Zhu XL, Li PT, Liu Y, Zhang N, Xu Y, Jia X (2009) The inhibitory effects of cholalic acid and hydoxycholalic acid on the expression of TNF-alpha and IL-1beta after cerebral ischemia in rats. *Arch Pharm Res* 32:65-73.
- Ibáñez CF, Andressoo JO (2017) Biology of GDNF and its receptors — Relevance for disorders of the central nervous system. *Neurobiol Dis* 97:80-89.
- Jijun C, Ai Qin W, Qingqi C (2016) Therapeutic indications and action mechanisms of bilirubin: suggestions from natural calculus bovis. *Curr Signal Transduct Ther* 11:13-22.
- Khoshnam SE, Winlow W, Farzaneh M, Farbood Y, Moghaddam HF (2017) Pathogenic mechanisms following ischemic stroke. *Neurol Sci* 38:1167-1186.
- Kowiański P, Lietzau G, Czuba E, Waśkow M, Steliga A, Moryś J (2018) BDNF: a key factor with multipotent impact on brain signaling and synaptic plasticity. *Cell Mol Neurobiol* 38:579-593.
- Le Moan N, Leung PY, Rost N, Winger JA, Krtolica A, Cary SP (2017) A new paradigm in protecting ischemic brain: preserving the neurovascular unit before reperfusion. In: *Neuroprotective therapy for stroke and ischemic disease* (Lapchak PA, Zhang JH, eds), pp 641-664. Cham: Springer International Publishing.
- Leng T, Liu A, Wang Y, Chen X, Zhou S, Li Q, Zhu W, Zhou Y, Su X, Huang Y, Yin W, Qiu P, Hu H, Xiong ZG, Zhang J, Yan G (2016) Naturally occurring marine steroid 24-methylenecholestane-3beta,5alpha,6beta,19-tetraol functions as a novel neuroprotectant. *Steroids* 105:96-105.
- Liao LX, Zhao MB, Dong X, Jiang Y, Zeng KW, Tu PF (2016) TDB protects vascular endothelial cells against oxygen-glucose deprivation/reperfusion-induced injury by targeting miR-34a to increase Bcl-2 expression. *Sci Rep* 6:37959.
- Liu D, Zhang M, Rong X, Li J, Wang X (2017) Potassium 2-(1-hydroxypentyl)-benzoate attenuates neuronal apoptosis in neuron-astrocyte co-culture system through neurotropy and neuroinflammation pathway. *Acta Pharm Sin B* 7:554-563.
- Liu J, Wang YH, Li W, Liu L, Yang H, Meng P, Han YS (2019) Structural and functional damage to the hippocampal neurovascular unit in diabetes-related depression. *Neural Regen Res* 14:289-297.
- Liu Q, Hou J, Chen X, Liu G, Zhang D, Sun H, Zhang J (2014) P-glycoprotein mediated efflux limits the transport of the novel anti-Parkinson's disease candidate drug FLZ across the physiological and PD pathological in vitro BBB models. *PLoS One* 9:e102442.
- Liu R, Zhang TT, Wu CX, Lan X, Du GH (2011) Targeting the neurovascular unit: development of a new model and consideration for novel strategy for Alzheimer's disease. *Brain Res Bull* 86:13-21.
- Liu Z, Chopp M (2016) Astrocytes, therapeutic targets for neuroprotection and neurorestoration in ischemic stroke. *Prog Neurobiol* 144:103-120.
- Morrison HW, Filosa JA (2019) Stroke and the neurovascular unit: glial cells, sex differences, and hypertension. *Am J Physiol Cell Physiol* 316:C325-339.
- Ovbiagele B, Goldstein LB, Higashida RT, Howard VJ, Johnston SC, Khavjou OA, Lackland DT, Lichtman JH, Mohl S, Sacco RL, Saver JL, Trogon JG; American Heart Association Advocacy Coordinating Committee and Stroke Council (2013) Forecasting the future of stroke in the United States: a policy statement from the American Heart Association and American Stroke Association. *Stroke* 44:2361-2375.
- Park H, Ahn SH, Jung Y, Yoon JC, Choi YH (2017) Leptin suppresses glutamate-induced apoptosis through regulation of ERK1/2 signaling pathways in rat primary astrocytes. *Cell Physiol Biochem* 44:2117-2128.
- Quan Z, Quan Y, Wei B, Fang D, Yu W, Jia H, Quan W, Liu Y, Wang Q (2015) Protein-protein interaction network and mechanism analysis in ischemic stroke. *Mol Med Rep* 11:29-36.
- Saarma M, Sariola H (1999) Other neurotrophic factors: glial cell line-derived neurotrophic factor (GDNF). *Microsc Res Tech* 45:292-302.
- Schmidt A, Minnerup J (2016) Promoting recovery from ischemic stroke. *Expert Rev Neurother* 16:173-186.
- Shaikh IH, Miah MK, Bickel U, Mehvar R (2013) Effects of short-term portacaval anastomosis on the peripheral and brain disposition of the blood-brain barrier permeability marker sodium fluorescein in rats. *Brain Res* 1531:84-93.
- Shi L, Cao HM, Li Y, Xu SX, Zhang Y, Zhang Y, Jin ZF (2017) Electroacupuncture improves neurovascular unit reconstruction by promoting collateral circulation and angiogenesis. *Neural Regen Res* 12:2000-2006.
- Shih DM, Shaposhnik Z, Meng Y, Rosales M, Wang X, Wu J, Ratiner B, Zadini F, Zadini G, Lusic AJ (2013) Hydoxycholeic acid improves HDL function and inhibits atherosclerotic lesion formation in LDLR-knockout mice. *FASEB J* 27:3805-3817.
- Tejeda GS, Diaz-Guerra M (2017) Integral characterization of defective bdnf/trkb signalling in neurological and psychiatric disorders leads the way to new therapies. *Int J Mol Sci* 18.
- Tian X, Peng J, Zhong J, Yang M, Pang J, Lou J, Li M, An R, Zhang Q, Xu L, Dong Z (2016) beta-Caryophyllene protects in vitro neurovascular unit against oxygen-glucose deprivation and re-oxygenation-induced injury. *J Neurochem* 139:757-768.
- Tschirner A, von Haehling S, Palus S, Doehner W, Anker SD, Springer J (2012) Ursodeoxycholic acid treatment in a rat model of cancer cachexia. *J Cachexia Sarcopenia Muscle* 3:31-36.
- Wu KW, Kou ZW, Mo JL, Deng XX, Sun FY (2016) Neurovascular coupling protects neurons against hypoxic injury via inhibition of potassium currents by generation of nitric oxide in direct neuron and endothelium cocultures. *Neuroscience* 334:275-282.
- Xing C, Hayakawa K, Lok J, Arai K, Lo EH (2012) Injury and repair in the neurovascular unit. *Neurol Res* 34:325-330.
- Xu XL, Ma CY, Wang XQ, Wang GL, Zhai CM, Yue WC, Li CX, Zhang XY, Shen XD, Mu J, Wang QG, Cheng FF (2017) Comparative study of cholic acid compounds of bezoar on anti-cerebral infarction and regulating endoplasmic reticulum stress. *Yaowu Pingjia Yanjiu* 40:11-19.
- Xue Q, Liu Y, Qi H, Ma Q, Xu L, Chen W, Chen G, Xu X (2013) A novel brain neurovascular unit model with neurons, astrocytes and micro-vascular endothelial cells of rat. *Int J Biol Sci* 9:174-189.

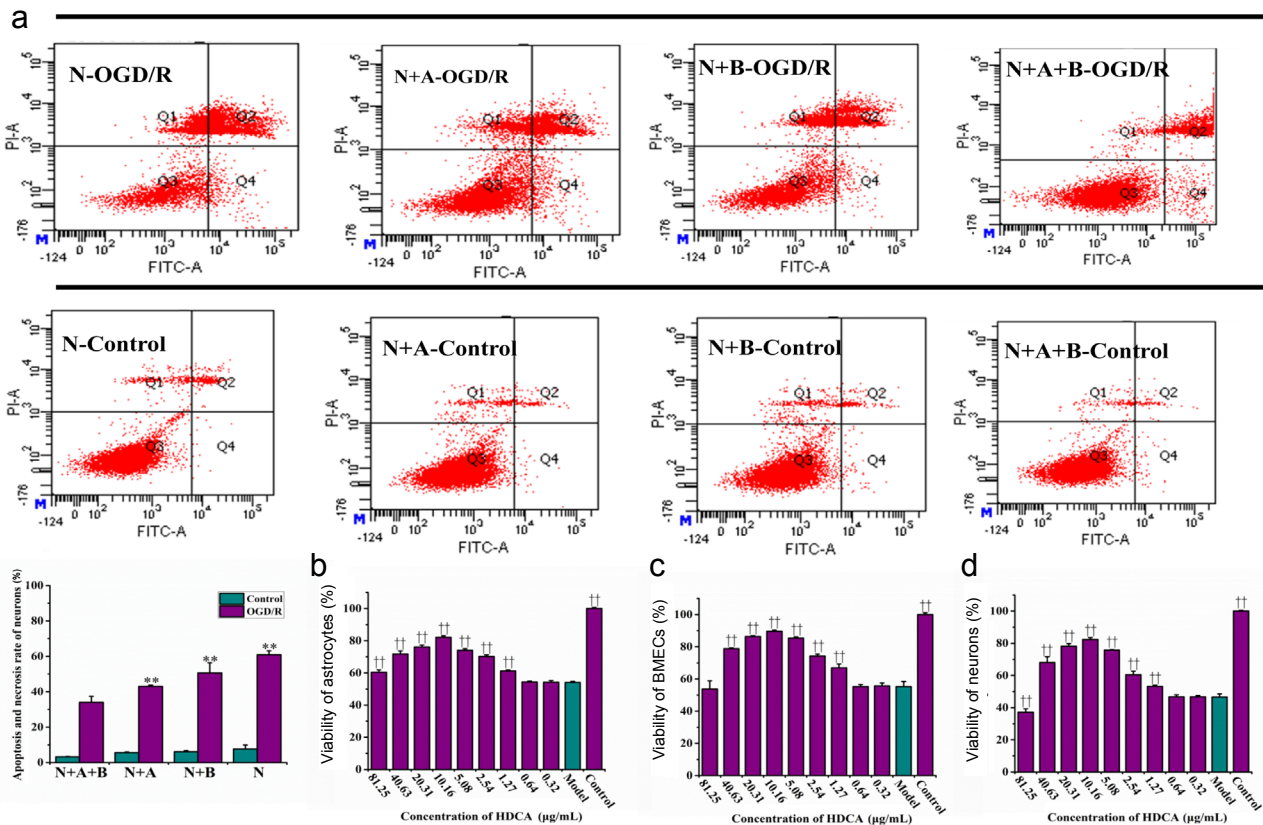


Figure 3 Protective effects of hydoxycholeic acid (HDCA) on astrocytes and neurons in the NVU exposed to oxygen-glucose deprivation and reoxygenation (OGD/R).

(a) Flow cytometry images indicating neuronal apoptosis and necrosis in the N, N + A, N + B and N + A + B groups. (b) Cell viability counts indicating the protective effects of HDCA on astrocytes after OGD (1 hour)/R (24 hours). (c) Cell viability counts indicating the protective effects of HDCA on BMECs after OGD (1 hour)/R (24 hours). (d) Cell viability counts showing the protective effects of HDCA on neurons after OGD (1 hour)/R (24 hours). Data are expressed as the mean ± SD. ** $P < 0.01$, vs. B + A + N group; †† $P < 0.01$, vs. model group (one-way analysis of variance followed by the least significant difference test). All experiments were performed in triplicate. B + A + N group: BMECs cultured with astrocytes and neurons; B + A group: BMECs cultured with astrocytes; B + N group: BMECs cultured with neurons; B group: BMECs cultured alone on the transwell chamber; N: neurons cultured alone on the transwell chamber; N + A group: neurons cultured with astrocytes; control: NVU system; model: NVU system exposed to OGD (1 hour)/R (24 hours); Q1 quadrant: necrosis; Q2 quadrant: early apoptosis; Q3 quadrant: normal cells; Q4 quadrant: late apoptosis.

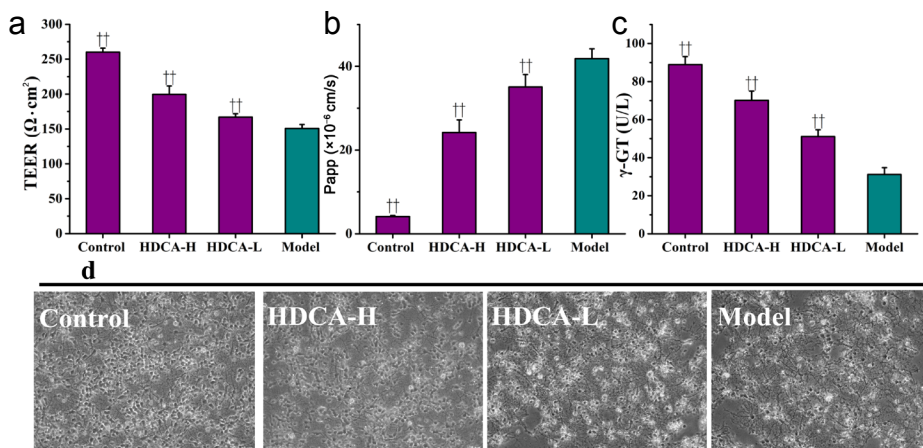


Figure 4 Dose-dependent effects of HDCA on blood-brain barrier (BBB) function and neuronal morphology after OGD/R.

(a) The effects of HDCA on the transendothelial electrical resistance (TEER) after OGD/R in the NVU system. The overall resistance can indicate the formation of a tight endothelial cell monolayer. (b) The effects of HDCA on the apparent permeability (Papp) after OGD/R in the NVU system. The Papp indicates the formation of tight junctions by BMECs (c) The effects of HDCA on γ -glutamyltransferase (γ -GT) after OGD/R in the NVU system. (d) The effects of HDCA on neuronal morphology after OGD/R in the NVU system. Scale bars: 20 μ m. Data are expressed as the mean ± SD. †† $P < 0.01$, vs. model group (one-way analysis of variance followed by the least significant difference test). All experiments were performed in triplicate. Control: NVU system; model: NVU system exposed to OGD (1 hour)/R (24 hours); HDCA-H and HDCA-L: NVU system exposed to OGD/R and pretreated with 10.16 μ g/mL or 2.54 μ g/mL HDCA for 24 hours.

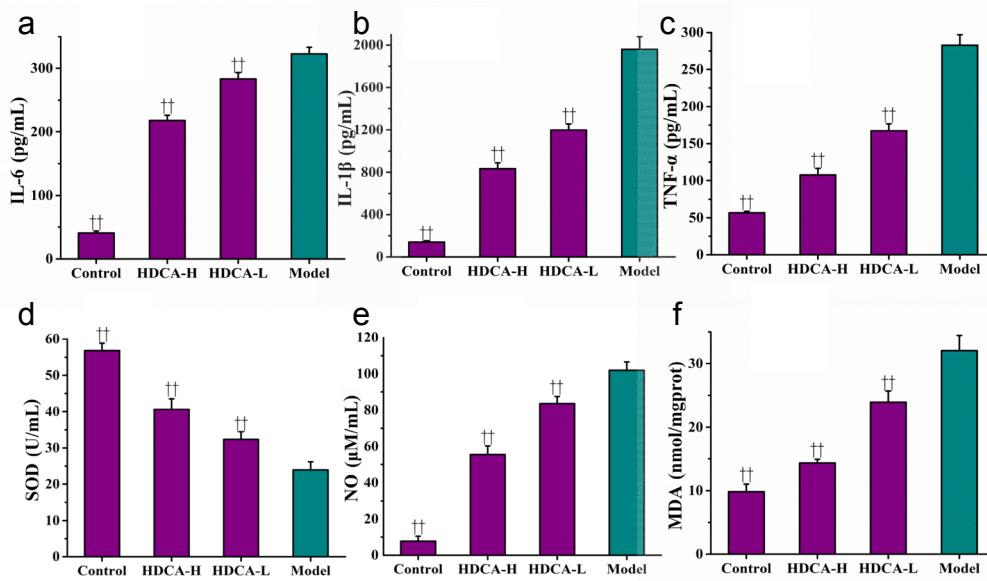


Figure 5 Effects of HDCA on inflammation and oxidative damage to the NVU model after OGD/R.

(a–f) Levels of inflammatory factors, interleukin (IL)-6, IL-1β and tumor necrosis factor-α (TNF-α), and biomarkers of oxidative stress, superoxide dismutase (SOD), NO and malondialdehyde (MDA). Data are expressed as the mean ± SD. ††*P* < 0.01, vs. model group (one-way analysis of variance followed by the least significant difference test). All experiments were performed in triplicate. Control: NVU system; model: NVU system subjected to OGD (1 hour)/R (24 hours); HDCA-H and HDCA-L: NVU system subjected to OGD/R and pretreated with 10.16 μg/mL or 2.54 μg/mL HDCA for 24 hours.

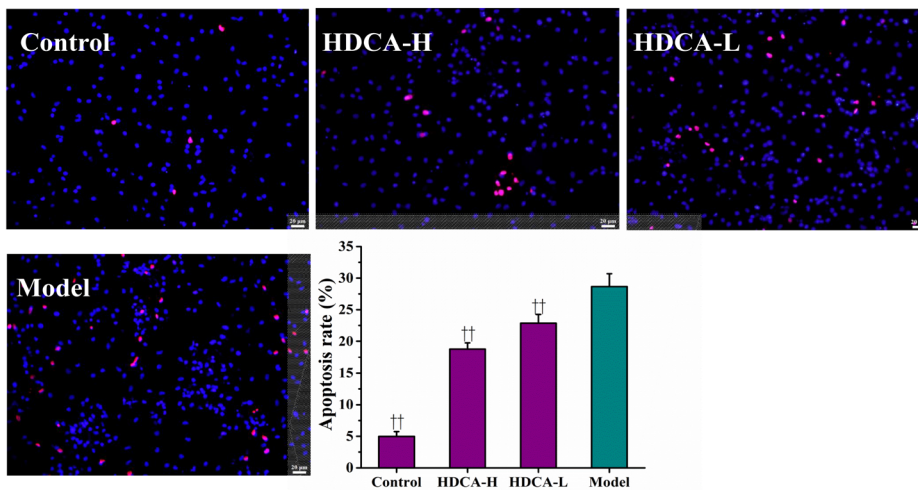


Figure 6 Effects of HDCA on apoptosis of neurons in the NVU model after OGD/R.

Representative images of cleaved-caspase 3 and TUNEL staining and quantification of the percentage of positive cells. Data are expressed as the mean ± SD. ††*P* < 0.01, vs. model group (one-way analysis of variance followed by the least significant difference test). All experiments were performed in triplicate. Control: NVU system; model: NVU system exposed to OGD (1 hour)/R (24 hours); HDCA-H and HDCA-L: NVU system subjected to OGD/R and pretreated with 10.16 μg/mL or 2.54 μg/mL HDCA for 24 hours.

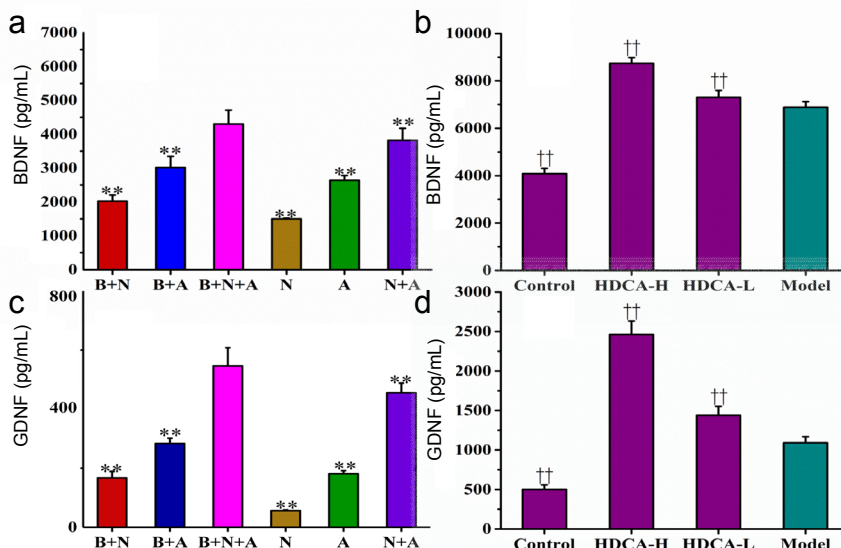


Figure 7 Effects of HDCA on BDNF and GDNF levels in the NVU model after OGD/R.

(a, c) The levels of BDNF and GDNF in the different culture systems. (b, d) Effects of HDCA on the expression of BDNF and GDNF. Data are expressed as the mean ± SD. ***P* < 0.01, vs. B + A + N group; ††*P* < 0.01, vs. model group (one-way analysis of variance followed by the least significant difference test). All experiments were performed in triplicate. B + A + N group: BMECs cultured with astrocytes and neurons; B + A group: BMECs cultured with astrocytes; B + N group: BMECs cultured with neurons; N: neurons cultured alone in the transwell chamber; A: astrocytes cultured alone in the transwell chamber; N + A: neurons cultured with astrocytes. Control: NVU system; model: NVU system exposed to OGD (1 hour)/R (24 hours); HDCA-H and HDCA-L: NVU system exposed to OGD/R and pretreated with 10.16 μg/mL or 2.54 μg/mL HDCA for 24 hours.